

## HOW MUCH IS RHIC DIFFERENT FROM SPS? COMPARISON OF THE $p_{\perp}$ -SPECTRA\*

WOJCIECH BRONIEWSKI AND WOJCIECH FLORKOWSKI

Henryk Niewodniczański Institute of Nuclear Physics  
Radzikowskiego 152, 31-342 Kraków, Poland

(Received April 9, 2002)

We show, by means of a simple compilation of the available experimental results, that the  $p_{\perp}$ -spectra obtained at RHIC and SPS are strikingly similar up to  $p_{\perp} \simeq 1.5\text{--}2$  GeV. Our observation is complementary to the well known fact of the equality of the measured  $R_{\text{side}}$  and  $R_{\text{out}}$  HBT radii at RHIC and SPS. In essence, it points out that the transverse size of the firecylinder and the strength of the transverse flow are not significantly changed between SPS and RHIC. This suggests that a saturation mechanism is effective already at SPS. We also point out that the dominance of protons over  $\pi^+$  at large  $p_{\perp}$  can be seen already in the SPS data.

PACS numbers: 25.75.-q, 25.75.Dw, 25.75.Ld

### 1. Introduction

The pertinent question in the field of relativistic heavy-ion collisions is whether the physics at RHIC is *qualitatively different* from the physics at SPS. In our opinion, the available experimental results hint that this is not the case, at least for soft processes.

In this paper we compile the transverse-momentum spectra of hadrons measured by various groups at SPS and RHIC. Surprisingly, to our knowledge such a study has not been presented before. We use the data of NA44 [1], NA49 [2], PHENIX [3], and STAR [4–6], and show that there exist discrepancies between the NA44 and the NA49 data, as well as between the PHENIX and the STAR data. In fact, these discrepancies are of the same size as the differences between SPS and RHIC. More precisely, within the experimental uncertainties, which are quite large, one finds that the slopes of the  $p_{\perp}$ -spectra at RHIC are compatible with those at SPS.

---

\* Supported by the Polish State Committee for Scientific Research (KBN), grant 2 P03B 09419.

This observation is complementary to the well known fact of the very weak beam-energy dependence of the transverse HBT radii. Similarity of both, the transverse size and the  $p_{\perp}$ -spectra of hadrons, indicates that the amount of the transverse flow cannot be significantly different at the two considered collision energies.

The transverse HBT radii  $R_{\text{side}}$  and  $R_{\text{out}}$  measured [7–9] in the first run of RHIC are very close to those measured in heavy-ion collisions at smaller beam energies. Only the longitudinal radius  $R_{\text{long}}$  exhibits a monotonic growth with  $\sqrt{s_{NN}}$  (for a compilation of the data at different energies see, *e.g.*, Ref. [7]). The weak energy dependence of the transverse radii is surprising, since the RHIC beam energy,  $\sqrt{s_{NN}} = 130$  GeV, is almost one order of magnitude larger than the SPS energy,  $\sqrt{s_{NN}} = 17$  GeV, and one would naively expect that much larger hadronic systems were produced at RHIC. One would also expect a longer lifetime of the hadronic fireball formed at RHIC, which should be reflected in a longer emission times of pions. This effect is quantified by the measurement of the ratio  $R_{\text{out}}/R_{\text{side}}$ , which is expected to be much larger than unity for long emission duration [10]. The experimental measurements indicate, however, that  $R_{\text{out}}/R_{\text{side}}$  is compatible with unity in the whole range of the studied transverse-momentum range ( $0.2 < k_{\text{T}} < 1.0$  GeV). This fact is another puzzle of the analysis of the RHIC data.

On the other hand, the first measurements at RHIC showed that the pseudorapidity densities of charged particles are higher than those observed at SPS. Can this effect be reconciled with practically unchanged transverse radii? For the most central collisions, PHOBOS communicated the value  $\langle N_{\text{ch}} \rangle = 555 \pm 12 \pm 35$  [11], BRAHMS the value  $\langle N_{\text{ch}} \rangle = 549 \pm 1 \pm 35$ , whereas PHENIX obtained  $\langle N_{\text{ch}} \rangle = 622 \pm 1 \pm 41$  [12]. Normalizing per participant pair yields  $\langle N_{\text{ch}} \rangle / (0.5 \langle N_{\text{part}} \rangle) = 3.2$  for both PHOBOS and BRAHMS, and  $\langle N_{\text{ch}} \rangle / (0.5 \langle N_{\text{part}} \rangle) = 3.6$  for PHENIX. These numbers may be compared to the NA49 result, 1.9 [11, 13], and the WA98 result, 2.6 [14]. We can see that the multiplicity increases by about 50% when we move from SPS to RHIC. A simple geometric scaling suggests that the transverse radius increases, correspondingly, as a square root, *i.e.*, by about 20%. Thus, the observed increase of the multiplicity translates to moderately small increase of the transverse radii. Clearly, the difference between the NA49 multiplicity and the WA98 multiplicity, as well as the errors of each particular experiment, lead to the uncertainty in the determination of the geometric parameters.

The weak dependence of  $R_{\text{side}}$  from SPS to RHIC means that the transverse size of the firecylinder changes very little. If this is the fact, than the amount of the transverse hydrodynamic flow should also be similar, since it is difficult to imagine that a much stronger flow would lead to the same transverse size at freeze-out. To the contrary, the STAR results for the

$p_{\perp}$ -spectra have been interpreted as an indication of a much stronger flow at RHIC. Below we redo the simple analysis of the hadronic spectra and show that the errors in the flow parameter are very large, such that one cannot definitely conclude that the flow is stronger at RHIC. Moreover, the PHENIX data suggest a much lower flow than STAR, such that it becomes compatible with the flow at SPS, as obtained from NA44 and NA49.

## 2. Compilation of the $p_{\perp}$ -spectra measured at SPS and RHIC

We begin by just displaying the experimental results from various groups in a single plot. In Fig. 1 we plot the  $p_{\perp}$ -spectra of  $\pi^{-}$ ,  $K^{-}$ ,  $\bar{p}$ , and  $\bar{\Lambda}$ . Similarly, in Fig. 2 we show the  $p_{\perp}$ -spectra of  $\pi^{+}$ ,  $K^{+}$ ,  $p$ , and  $\Lambda$ . The collected data come from the measurements done at midrapidity for the most central events [1–6]. A striking feature of Fig. 1 is a very impres-

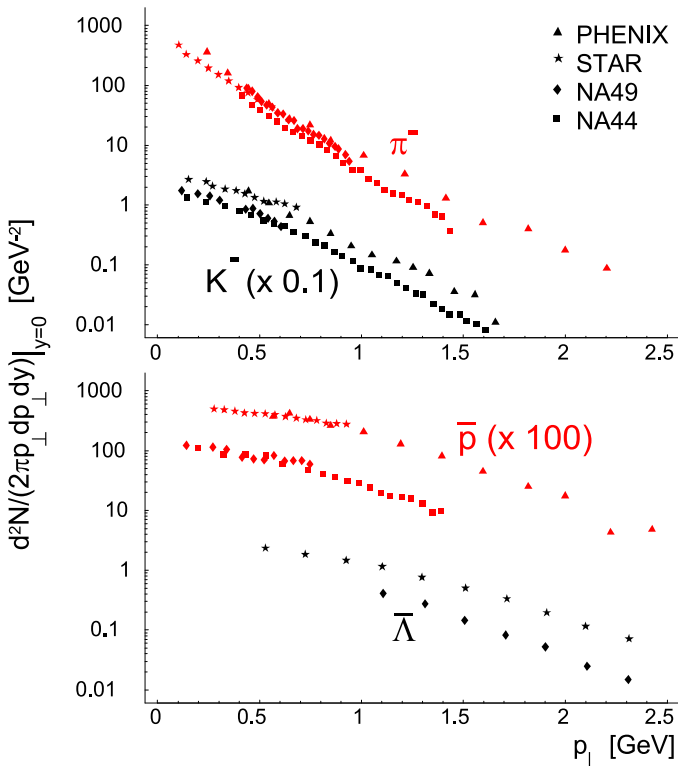


Fig. 1. Comparison of the mid-rapidity  $p_{\perp}$ -spectra of  $\pi^{-}$ ,  $K^{-}$ ,  $\bar{p}$ , and  $\bar{\Lambda}$  for the most central collisions of Pb+Pb at  $\sqrt{s_{NN}} = 17$  GeV (NA44, NA49) and Au+Au at  $\sqrt{s_{NN}} = 130$  GeV (PHENIX, STAR). The STAR data for  $\pi^{-}$  and  $K^{-}$ , and the NA49 data are preliminary.

sive agreement between different experiments for the pions. In the range  $0.4 < p_{\perp} < 1.0$  GeV, the data from NA49 coincide with the data from PHENIX and STAR, whereas the data from NA44 show the same slope with a slightly smaller normalization due to a different centrality choice (see the discussion below). A very similar  $p_{\perp}$ -dependence is also seen in the spectra of kaons,  $\bar{p}$ , and  $\bar{\Lambda}$  measured by different experiments. In this case, however, a different normalization of the spectra between SPS and RHIC data is clearly seen. In Fig. 2 one can clearly see similarities in the shapes of the pion as well as the kaon spectra measured by NA44 and PHENIX.

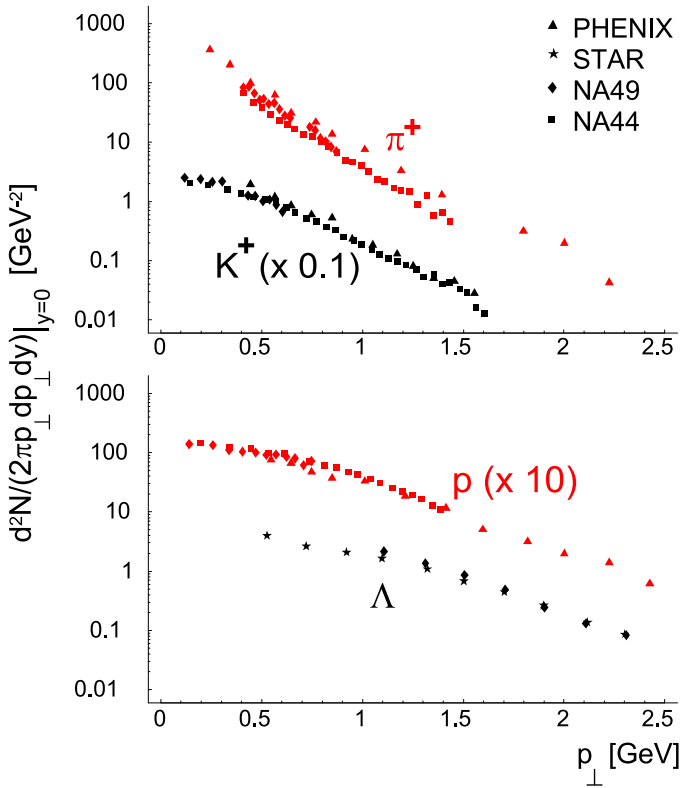


Fig. 2. Same as Fig. 1 for  $\pi^+$ ,  $K^+$ ,  $p$ , and  $\Lambda$ .

If the plots for mesons and baryons were overlaid (*cf.* [15,16]), one could see that the PHENIX data have the property that the  $p_{\perp}$ -spectra of  $\pi^+$  and  $p$  cross around  $p_{\perp} = 2$  GeV, such that there are more protons than  $\pi^+$  at large momenta. We wish to stress that the same phenomenon can be seen already at SPS, where the protons dominate  $\pi^+$  at  $p_{\perp} > 1$  GeV. The lower value of the crossing point reflects a much higher proton density at SPS compared to RHIC.

At RHIC, the “anomalous” [3, 17] feature of the spectra is the dominance of  $\bar{p}$  over  $\pi^-$  at  $p_\perp > 2$  GeV. One could speculate that a similar behavior might occur already at SPS, if the measurements had been carried out to sufficiently high momenta. Indeed, when the NA44 data are extrapolated with simple exponential functions, then one finds that a crossing occurs around  $p_\perp = 2.5$  GeV. Since the exponential fits may not work over the large range in  $p_\perp$ , this phenomenon remains a speculation till verified experimentally.

In order to see the similarities between the data even more vividly, we scale the normalization of the spectra in the following way:

1. In the NA49 data we undo the corrections for the feeding of protons and antiprotons from weak decays. According to Ref. [2], this correction is about 30%, thus we divide the NA49 data for  $p$  and  $\bar{p}$  by the factor 0.7.
2. The most central data from NA44 correspond to the average impact parameter  $\langle b \rangle = 5$  fm, whereas the most central NA49 data correspond to  $\langle b \rangle = 2$  fm [1]. This difference explains a smaller normalization of the NA44 data. We correct for the centrality choice of NA44, multiplying all NA44 spectra by an educated-guess factor of 1.5.
3. Inspired by the success of the thermal approach, we scale the spectra by the factor  $\exp[-(B\mu_B + S\mu_S + I_3\mu_I)/T]$ , where  $T$  is the freeze-out temperature,  $B$ ,  $S$ , and  $I_3$  are the baryon number, strangeness, and the third component of the isospin of the particle, respectively, and  $\mu_B$ ,  $\mu_S$ , and  $\mu_I$  are the corresponding chemical potentials. At SPS (Pb+Pb,  $\sqrt{s_{NN}} = 17$  GeV) [18]

$$T = 164 \text{ MeV}, \quad \mu_B = 229 \text{ MeV}, \quad \mu_S = 54 \text{ MeV}, \quad \mu_I = -7 \text{ MeV}, \quad (1)$$

while at RHIC (Au+Au,  $\sqrt{s_{NN}} = 130$  GeV) [19]

$$T = 165 \text{ MeV}, \quad \mu_B = 41 \text{ MeV}, \quad \mu_S = 9 \text{ MeV}, \quad \mu_I = -1 \text{ MeV}. \quad (2)$$

Since in the thermal model the (original) spectra are proportional to the factor  $\exp[(B\mu_B + S\mu_S + I_3\mu_I)/T]$  (for the Boltzmann statistics, which works very well), our rescaling approximately removes the effects of different chemical potentials at RHIC and SPS. Due to resonance decays, even within the thermal model the scaling is not exact, but approximate<sup>1</sup>.

---

<sup>1</sup> For instance, a larger baryon chemical potential leads to a larger pion yield from the process  $\Delta \rightarrow \pi N$ , hence the secondary pions are sensitive to the baryon chemical potential.

The described rescaling is not necessary for our analysis, and has no impact on the conclusions. However, it is useful, since it brings the spectra closer and makes the eye-ball comparison easier. The results are shown in Figs. 3 and 4. For the pions, the four measurements agree very well in the overlap region. For the kaons, the NA49 data have a visibly larger slope, while the three other sets of data overlap. The measurements for protons and  $\bar{p}$  agree as well. The spectra of  $\Lambda$  and  $\bar{\Lambda}$  have smaller slopes in the STAR measurement compared to NA49. One should bare in mind that the statistical errors are typically of the order of a few percent, and the systematic errors are around 10%. Hence, within the experimental errors, there are no significant differences between SPS and RHIC which could indicate different physics. Moreover, the small difference between NA44 and NA49, and between PHENIX and STAR, which one may observe in Figs. 3 and 4 is of the same magnitude as the difference between SPS and RHIC.

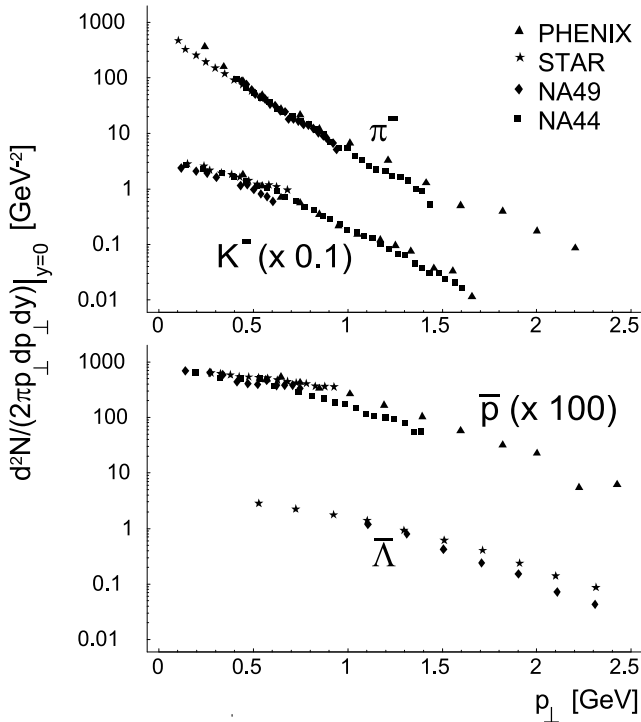


Fig. 3. Same as Fig. 1 for the rescaled spectra.

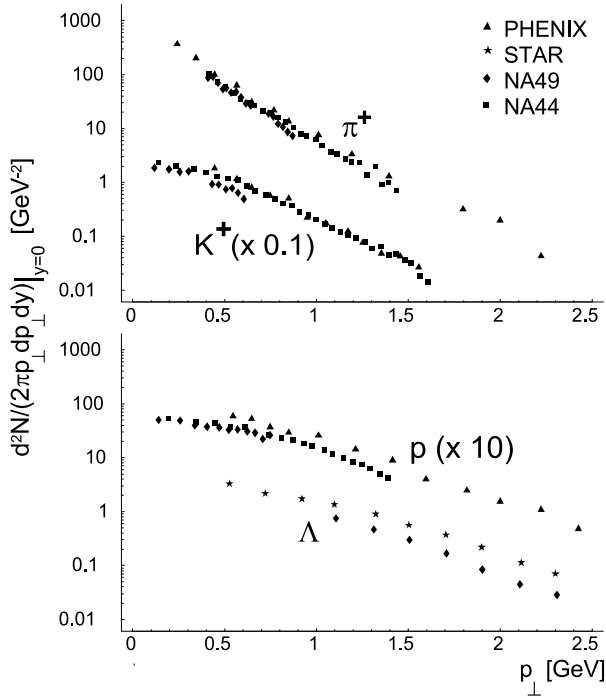


Fig. 4. Same as Fig. 2 for the rescaled spectra.

### 3. Exponential fits

In this section we wish to quantify the eye-ball observations from Figs. 3 and 4. The most popular method is to fit the spectra to the exponential function, and compare the parameters. In fact, this is the most economic and common way of presenting the data, and the differences in the slope parameters of particles of different masses are interpreted as the signature of the transverse flow [20,21]. Hence, we fit the function<sup>2</sup>

$$\left. \frac{d^2N}{m_{\perp} dm_{\perp} dy} \right|_{y=0} = A \exp(-m_{\perp}/\lambda) \quad (3)$$

to each *rescaled* spectrum, independently for different experimental groups<sup>3</sup>. The method is as follows: we constrain the fit to  $p_{\perp} < 2\text{GeV}$  (this has

<sup>2</sup> Other forms used in the literature, differing by the power of  $m_{\perp}$ , lead to similar qualitative conclusions.

<sup>3</sup> We note that the slope parameters,  $\lambda$ , fitted in many papers, depend strongly on the choice of the range in  $p_{\perp}$  (see, *e.g.*, the discussion in [22]). Here we use the available data ranges with  $p_{\perp} < 2\text{GeV}$ . Because of the lack of strict thermodynamic interpretation, we refrain from calling  $\lambda$  the temperature of the spectrum.

relevance for the PHENIX data, and for  $A$  and  $\bar{A}$  measured by STAR). For simplicity, we assume a 15% error on every point. This is in the ballpark of the errors given by the experimental groups. Then, the  $\chi^2$  function is minimized with respect to the  $A$  and  $\lambda$  parameters.

The results are shown in Fig. 5. The first feature to notice are large correlations between  $\lambda$  and  $A$ , which lead to sizeable errors in these parameters. The optimum values for  $\lambda$ , denoted in Fig. 5 by crosses, and the errors are

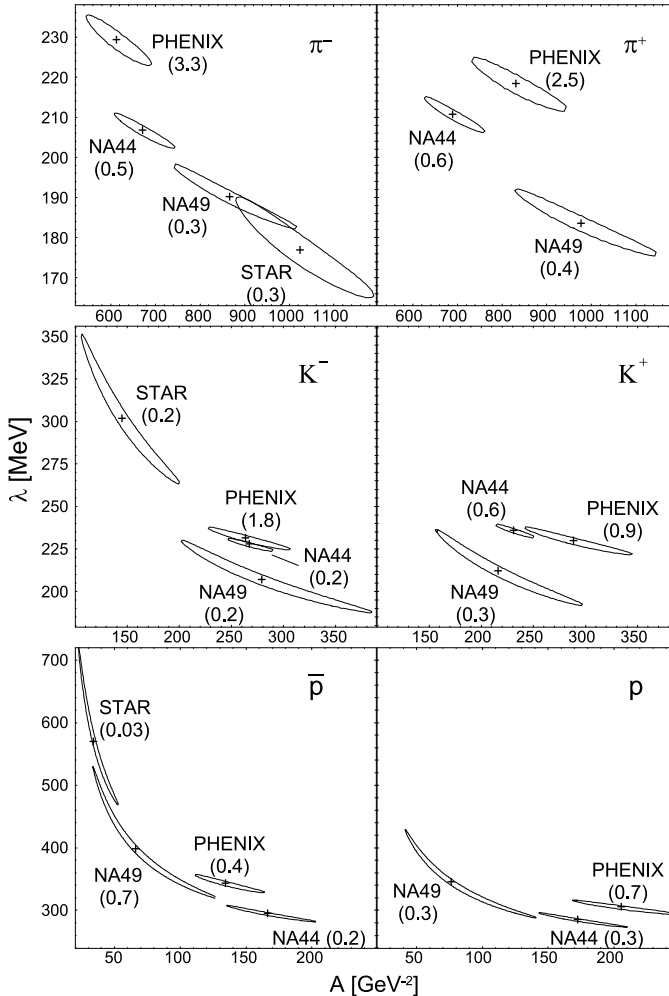


Fig. 5. The contours of  $\Delta\chi^2 = 1$  for various fits of the rescaled mid-rapidity  $p_{\perp}$ -spectra to the exponential form  $A \exp(-m_{\perp}/\lambda)$ . Optimum values are denoted by crosses. The numbers in parentheses are the values of the  $\chi^2$  per degree of freedom at the optimum. The data for NA49 and the STAR data for  $\pi^-$  and  $K^-$  are preliminary.



listed in Table I. While the optimum values agree with the estimates made in other papers [1–4], our errors are significantly larger for the case of STAR and NA49. The physically relevant parameter is the inverse slope,  $\lambda$ , while the norm parameter,  $A$ , carries the ambiguities described above (rescaling). Hence, if the results of the two data sets are to be consistent, then the ranges of  $\lambda$  (and not necessarily  $A$ ) should overlap. We note from Fig. 5 that this is basically the case for NA44 and NA49, except perhaps the case of  $\pi^+$ . The STAR and PHENIX data are much less consistent, especially for the case of  $\pi^-$ . For kaons, protons, and  $\bar{p}$ , the PHENIX data agree within errors with NA44 and NA49. Some caution is needed in the interpretation of Fig. 5, since the fits are made over different ranges in  $p_\perp$ , and the form used for the fit has no sound physical ground. Yet, there are indications for discrepancies between STAR and PHENIX. Also, it is clear that only the STAR data suggest larger values of  $\lambda$  (albeit with large errors), which would mean larger transverse flow. If PHENIX data are used, no such conclusion comes out, since the PHENIX data are basically consistent with SPS. Note also that the quality of the fit, indicated by the value of  $\chi^2$  at the optimum, is worst for the case of pions from PHENIX. This reflects the inapplicability of the simple exponential parameterization over the large range in  $p_\perp$ .

TABLE I

Our values for the inverse-slope parameters,  $\lambda$ , in units of MeV, fitted to mid-rapidity data from the most-central collisions of Pb+Pb at  $\sqrt{s_{NN}} = 17$  GeV (NA44 [1], NA49 [2]) and Au + Au at  $\sqrt{s_{NN}} = 130$  GeV (PHENIX [3], STAR [4–6]). The fit includes data points up to 2 GeV. The NA49 data, and the STAR data for  $\pi^-$  and  $K^-$  are preliminary.

	NA44	NA49	PHENIX	STAR
$\pi^+$	$211 \pm 4$	$183 \pm 8$	$218 \pm 7$	
$\pi^-$	$207 \pm 4$	$190 \pm 8$	$229 \pm 6$	$176 \pm 12$
$K^+$	$235 \pm 4$	$211 \pm 22$	$230 \pm 8$	
$K^-$	$227 \pm 4$	$207 \pm 21$	$231 \pm 7$	$301 \pm 43$
$p$	$284 \pm 12$	$344 \pm 68$	$304 \pm 12$	
$\bar{p}$	$294 \pm 14$	$397 \pm 100$	$342 \pm 15$	$569 \pm 122$
$A$		$294 \pm 24$		$372 \pm 22$
$\bar{A}$		$298 \pm 27$		$398 \pm 25$

The final remark of this section concerns the multiplicities of particles,

$$\left. \frac{dN}{dy} \right|_{y=0} = \int_0^{\infty} dp_{\perp} p_{\perp} \left. \frac{d^2N}{p_{\perp} dp_{\perp} dy} \right|_{y=0}. \quad (4)$$

The integrand in Eq. (4) peaks at  $p_{\perp} \simeq 0.25$  GeV for the pions, and 0.6 GeV for the protons. Therefore, much of the strength comes from the  $p_{\perp}$  region not covered by the data. The necessary extrapolation brings systematic uncertainties to  $dN/dy$  and may be a source of discrepancies between various quoted numbers.

#### 4. A model calculation

The estimates of the transverse flow must be based on model calculations which include this effect, as well as other potentially important physical effects. In this section we apply the *single-freeze-out model*, which has been used successfully to describe the  $p_{\perp}$ -spectra at RHIC. The model has been described in detail in Refs. [15, 16, 22], and here we only list its basic features: (i) simultaneous chemical and thermal freeze-out of the hadronic matter, (ii) inclusion of all hadronic resonances, and (iii) a simple parametrization of the freeze-out hypersurface, which is defined by the condition  $\tau = \sqrt{t^2 - x^2 - y^2 - z^2} = \text{const}$ . The hydrodynamic flow on the freeze-out hypersurface is taken in the form resembling the Hubble law, *i.e.*,  $u^{\mu} = x^{\mu}/\tau$ . That way both the longitudinal and transverse flows are built in. The single-freeze-out model has two thermodynamic parameters (temperature and the baryon chemical potential) which are fixed by the global fit to the relative particle yields (*cf.* Eqs. (1), (2)). The extra two parameters ( $\tau$  and the transverse radius of the firecylinder  $\rho_{\text{max}}$ ) determine the overall normalization and the shape of the spectra. In our present calculation the thermodynamic parameters are the same as those used previously in Sect. 2<sup>4</sup>. Then, the expansion parameters  $\tau$  and  $\rho_{\text{max}}$  are fixed separately to the data of each experimental group. They determine, in each particular case, the maximal transverse flow, given by the model formula

$$\beta_{\perp}^{\text{max}} = \frac{\rho_{\text{max}}}{\sqrt{\tau^2 + \rho_{\text{max}}^2}}. \quad (5)$$

The average value of the transverse flow velocity,  $\langle \beta_{\perp} \rangle$ , is very close to  $(2/3) \beta_{\perp}^{\text{max}}$ .

---

<sup>4</sup> We note that  $T$  and  $\mu_B$  are the only independent thermodynamic parameters, since  $\mu_S$  and  $\mu_I$  follow from the conservation of strangeness and electric charge.

The results are presented in Fig. 6, where we show the optimum values for the invariant time,  $\tau$ , and the flow parameter,  $\beta_{\perp}^{\max}$ , together with their errors. If the results were internally consistent, the fitted values would overlap. This is not the case. The fit to NA44 is far away from the fit to NA49, and the fit to STAR is far away from the fit to PHENIX. Amusingly, PHENIX is close to NA44, and STAR is close to NA49. The grand average of  $\beta_{\perp}^{\max}$  from combined PHENIX and STAR is close to the average from combined NA44 and NA49 experiments. These results indicate that even within a model capable of explaining the spectra one cannot conclude of a larger transverse flow at RHIC compared to SPS.

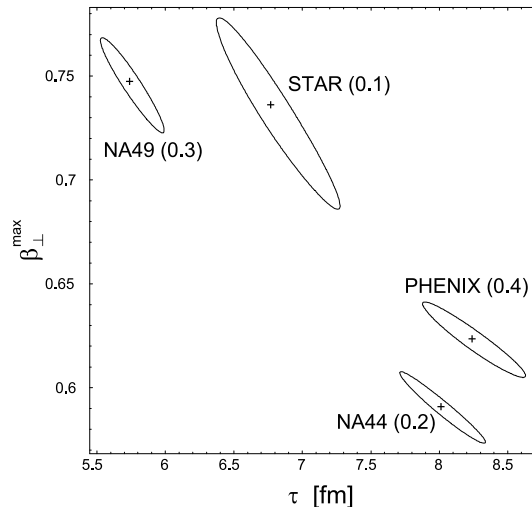


Fig. 6. The contours of  $\Delta\chi^2 = 1$  for fits of the combined mid-rapidity  $p_{\perp}$ -spectra to the *single-freeze-out model* of Refs. [15, 22]. The parameters  $\tau$  and  $\beta_{\perp}^{\max}$  are defined in the text. The optimum values of the parameters are denoted by crosses. The numbers in parentheses are the values of the  $\chi^2$  per degree of freedom at the optimum. The NA49 data and the STAR data for  $\pi^-$  and  $K^-$  are preliminary.

## 5. Conclusions

Here are our main points:

1. The similarity of  $p_{\perp}$ -spectra at SPS and RHIC in the data range suggests similar soft physics. We have argued that the combined present data do not lead to the conclusion of much larger transverse flow at RHIC. Only the STAR data for  $\bar{p}$  and  $K^-$  support this view, although with large experimental uncertainty. The PHENIX data are compatible with the same transverse flow as in SPS.

2. The property of the spectra that there are more protons than  $\pi^+$  at large  $p_{\perp}$  can be seen not only in the RHIC data, but also in the SPS data.
3. At the moment the experimental discrepancies between NA44 and NA49, and between STAR and PHENIX are of the same magnitude as the discrepancies between SPS and RHIC. With better data more accurate conclusion would be achieved. In particular, the RHIC measurements at lower energies will be very useful in verifying theoretical hypotheses. The use of models failing to reproduce the RHIC data should be, if possible, avoided in the modeling of detectors and in the analysis of the data. Also, the frequently made corrections for weak decays are not very useful, since these can be accounted for without difficulty in theoretical models. When comparing the corrected data much care is needed as to how the feeding from weak decays has been subtracted.
4. We recall that the freeze-out temperatures used in the framework of thermal models have saturated (compare Eqs. (1) and (2)), which was not yet the case at AGS energies. Note, however, that the thermal approach works well for the AGS data [23, 24] and for elementary collisions [25].
5. The transverse HBT radii and the slopes of the spectra are similar at SPS and RHIC, which implies similar transverse flow, or, in general, similar soft transverse physics. The particle yields increased by 50% from SPS to RHIC naturally result in 20% increase of the transverse size and flow. We also recall that the magnitude of the elliptic flow coefficient,  $v_2$ , is similar from SPS to RHIC [26].
6. The similarity of the soft physics at RHIC and SPS may be explained by the parton saturation phenomenon [27,28] (scenario (2) of Ref. [29]). If the onset of saturation occurs already at SPS energies, then the initial conditions for the multiparticle production are similar at SPS and RHIC, explaining the similarities discussed in this paper. The situation is reminiscent of the Hagedorn saturation [30–32] in elementary collisions, where the further increase of the collision energy does not lead to increased temperature.
7. The property of the saturation of soft physics, or at least the very weak dependence on the collision energy, should help to verify and constrain various models. The incomplete list of the most popular approaches and ideas includes: thermal models [15, 16, 19, 33–38], hydrodynamic models [39–49], transport theories [10], and saturation models [29].

## REFERENCES

- [1] I.G. Bearden *et al.*, NA44 Collaboration, nucl-ex/0202019, submitted to *Phys. Rev. C*.
- [2] P.G. Jones, NA49 Collaboration, *Nucl. Phys.* **A610**, 188c (1996).
- [3] K. Adcox *et al.*, PHENIX Collaboration, nucl-ex/0112006; J. Velkovska, PHENIX Collaboration, *Nucl. Phys.* **A698**, 507 (2002).
- [4] C. Adler *et al.*, STAR Collaboration, *Phys. Rev. Lett.* **87**, 262302 (2001).
- [5] J. Harris, STAR Collaboration, contribution to QM2001.
- [6] C. Adler *et al.*, STAR Collaboration, nucl-ex/0203016.
- [7] K. Adcox *et al.*, PHENIX Collaboration, nucl-ex/0201008.
- [8] C. Adler *et al.*, STAR Collaboration, *Phys. Rev. Lett.* **87**, 082301 (2001).
- [9] L. Ahle *et al.*, E-802 Collaboration, nucl-ex/0204001.
- [10] S. Soff, S.A. Bass, A. Dumitru, *Phys. Rev. Lett.* **86**, 3981 (2001)
- [11] B.B. Back *et al.*, PHOBOS Collaboration, *Phys. Rev. Lett.* **85**, 3100 (2000).
- [12] K. Adcox *et al.*, PHENIX Collaboration, *Phys. Rev. Lett.* **87**, 052301 (2001).
- [13] H. Appelshäuser *et al.*, NA49 Collaboration, *Phys. Rev. Lett.* **82**, 2471 (1999).
- [14] M.M. Aggarwal *et al.*, WA98 Collaboration, *Eur. Phys. J.* **C18**, 651 (2001).
- [15] W. Broniowski, W. Florkowski, *Phys. Rev. Lett.* **87**, 272302 (2001).
- [16] W. Broniowski, W. Florkowski, Proceedings of the International Workshop XXX on Gross Properties of Nuclei and Nuclear Excitations, Hirscheegg, Austria, GSI, Darmstadt, 2002, p. 146.
- [17] I. Vitev, M. Gyulassy, nucl-th/0104066.
- [18] M. Michalec, nucl-th/0112044.
- [19] W. Florkowski, W. Broniowski, M. Michalec, *Acta Phys. Pol.* **B33**, 761 (2002).
- [20] T. Csörgő, B. Lörstad, *Phys. Rev.* **C54**, 1390 (1996).
- [21] R. Scheibl, U. Heinz, *Phys. Rev.* **C59**, 1585 (1999).
- [22] W. Broniowski, W. Florkowski, nucl-th/0112043.
- [23] P. Braun-Munzinger, J. Stachel, J.P. Wessels, N. Xu, *Phys. Lett.* **B344**, 43 (1995); *Phys. Lett.* **B365**, 1 (1996).
- [24] J. Cleymans, D. Elliott, H. Satz, R.L. Thews, *Z. Phys.* **C74**, 319 (1997).
- [25] F. Becattini, L. Bellucci, G. Passaleva, *Nucl. Phys. Proc. Suppl.* **92**, 137 (2001).
- [26] S.A. Voloshin, Proceedings of the International Workshop XXX on Gross Properties of Nuclei and Nuclear Excitations, Hirscheegg, Austria, GSI, Darmstadt, 2002, p. 207.
- [27] K. Golec-Biernat, M. Wüsthoff, *Phys. Rev.* **D59**, 014017 (1999); *Phys. Rev.* **D60**, 114023 (1999); *Eur. Phys. J.* **C20**, 313 (2001).
- [28] E. Iancu, A. Leonidov, L. McLerran, Lectures given at the NATO Advanced Study Institute "QCD perspectives on hot and dense matter", Cargèse, Corsica, France, 2001, hep-ph/0202270.

- [29] D. Kharzeev, E. Levin, M. Nardi, [hep-ph/0111315](#).
- [30] R. Hagedorn, CERN preprint No. CERN-TH.7190/94 (1994), and references therein.
- [31] W. Broniowski, W. Florkowski, *Phys. Lett.* **B490**, 223 (2000).
- [32] W. Broniowski, in Proc. of Few-Quark Problems, Bled, Slovenia, July 8–15, 2000, eds. B. Golli, M. Rosina and S. Širca, p. 14, [hep-ph/0008122](#).
- [33] P. Braun-Munzinger, I. Heppe, J. Stachel, *Phys. Lett.* **B465**, 15 (1999).
- [34] M. Gaździcki, M.I. Gorenstein, *Phys. Rev. Lett.* **83**, 4009 (1999).
- [35] J. Rafelski, J. Letessier, *Phys. Rev. Lett.* **85**, 4695 (2000); [hep-ph/0112027](#).
- [36] F. Becattini, J. Cleymans, A. Keranen, E. Suhonen, K. Redlich, *Phys. Rev.* **C64**, 024901 (2001).
- [37] P. Braun-Munzinger, D. Magestro, K. Redlich, J. Stachel, *Phys. Lett.* **B518**, 41 (2001).
- [38] K.A. Bugaev, M. Gaździcki, M.I. Gorenstein, *Phys. Lett.* **B523**, 255 (2001).
- [39] P.J. Siemens, J. Rasmussen, *Phys. Rev. Lett.* **42**, 880 (1979); P.J. Siemens, J.I. Kapusta, *Phys. Rev. Lett.* **43**, 1486 (1979).
- [40] J.D. Bjorken, *Phys. Rev.* **D27**, 140 (1983).
- [41] G. Baym, B. Friman, J.-P. Blaizot, M. Soyeur, W. Czyż, *Nucl. Phys.* **A407**, 541 (1983).
- [42] E. Schnedermann, J. Sollfrank, U. Heinz, *Phys. Rev.* **C48**, 2462 (1993).
- [43] D.H. Rischke, M. Gyulassy, *Nucl. Phys.* **A697**, 701 (1996); *Nucl. Phys.* **A608**, 479 (1996).
- [44] R. Scheibl, U. Heinz, *Phys. Rev.* **C59**, 1585 (1999).
- [45] A. Ster, T. Csörgő, [hep-ph/0112064](#).
- [46] P. Huovinen, P.F. Kolb, U. Heinz, P.V. Ruuskanen, S.A. Voloshin, *Phys. Lett.* **B503**, 58 (2001).
- [47] D. Teaney, J. Lauret, E.V. Shuryak, *Phys. Rev. Lett.* **86**, 4783 (2001); *Nucl. Phys.* **A698**, 479 (2002).
- [48] T. Hirano, *Phys. Rev.* **C65**, 011901 (2002); T. Hirano, K. Morita, S. Muroya, C. Nonaka, [nucl-th/0110009](#).
- [49] U. Heinz, *Nucl. Phys.* **A661**, 140c (1999).